Journal of Organometallic Chemistry 694 (2009) 2185–2190

Contents lists available at ScienceDirect

Journal of Organometallic Chemistry

journal homepage: www.elsevier.com/locate/jorganchem

Mn(II) azamacrocyclic bromide complexes with different nuclearities

Laura Valencia [a,*], Paulo Pérez-Lourido [a], Rufina Bastida [b], Alejandro Macías [b]

[a] Departamento de Química Inorgánica, Facultad de Química, Universidade de Vigo, As Lagoas, Marcosende, 36310 Vigo, Pontevedra, Spain
[b] Departamento de Química Inorgánica, Universidad de Santiago de Compostela, Avda. de las Ciencias s/n 15782, Santiago de Compostela, La Coruña, Spain

ARTICLE INFO

Article history:
Received 12 January 2009
Received in revised form 16 February 2009
Accepted 23 February 2009
Available online 6 March 2009

Keywords:
Pyridyl macrocyclic ligand
Manganese(II) complex
Pendant-arm
X-ray structure

ABSTRACT

The coordination behaviour of a series of pyridyl azamacrocyclic ligands, some of them containing cyanomethyl and cyanoethyl pendant-arms, towards Mn(II) ion was studied. All the complexes were characterized by microanalysis, LSI mass spectrometry, IR, UV–Vis spectroscopy and magnetic measurements. Crystal structures of $[MnL^1][MnBr_4]$ (**1**), $[MnL^3][MnBr_4] \cdot 2CH_3CN$ (**3**), $[Mn_2L^5Br_4] \cdot 2CH_3CN$ (**5**) and $[Mn_2L^6Br_4]$ (**6**) complexes have been determined. The X-ray studies show the presence of an ionic mixed octahedral–tetrahedral complex for **1** and **2**, with the manganese ion of the cation complex, endomacrocyclicly coordinated by the six nitrogen donor atoms from the macrocyclic backbone in a distorted octahedral geometry. Instead, the complexes **5** and **6** are dinuclear, and both manganese ions are coordinated by one pyridinic and two amine nitrogen atoms from the macrocyclic backbone and two bromide ions, being the geometry around the metal better described as distorted square pyramidal. In all cases, the nitrile pendant-arms do not show coordination to the metal ion.

1. Introduction

The coordination chemistry of macrocyclic ligands have received an extensive attention during last decades due its considerable potential in such areas as catalysis, modelling of metalloenzyme, molecular recognition, etc. [1]. The introduction of pendant-arms into the macrocyclic framework can led to important changes in the control of the stability, selectivity, stereochemistry and certain thermodynamic parameters [2–5]. The ligands L^1 and L^4 (Scheme 1) are a sample of versatile macrocyclic polyamine ligands from which many other ligands have been derived by attaching functional groups on its backbone, and their metal complexes show interesting properties and functions [6–16].

We have previously reported a series of potential decadentate ligands (L^2, L^3, L^5 and L^6) by attaching four cyanomethyl or cyanoethyl groups to that macrocycles [17–20], which potentially provide six nitrogen donor atoms from the macrocyclic backbone and four N donors from the nitrile pendant-arms.

In other hand, it is well-known that high-spin manganese complexes are largely investigated due their importance in different areas such as materials chemistry, catalysis or biochemistry [21–25]. Manganese ion plays an important role in some enzymes of great biological importance in the living systems. We can emphasize between them, the manganese superoxide dismutase, which has been shown to contain a mononuclear manganese active site [26]; pseudocatalase which contains a dinuclear active site [27,28] or the tetranuclear manganese center in the active site of the photosystem II [29,30].

Hence, as part as our research in the macrocyclic coordination area, we described here the synthesis and the structural characterization of a series of mononuclear and dinuclear Mn(II) complexes with the hexaazamacrocycles L^1, L^4, and their cyanomethyl or cyanoethyl pendant-arms derived: L^2, L^3, L^5 and L^6.

2. Experimental

2.1. Chemicals and starting materials

The ligands L^1 and L^4 were prepared according to a modification of a literature method [31,32]. The ligands with nitrile pendant-arms (L^2, L^3, L^5 and L^6) were synthesized starting from the precursors L^1 and L^4 [17–19]. Hydrated bromide manganese (II) salt was commercial product (from Aldrich) and it was used without further purification. Solvents were of reagent grade and were purified by standard methods.

2.2. Physical measurements

Elemental analyses were performed in a Carlo-Erba EA microanalyser. LSI-MS were recorded using a Micromass Autospec spectrometer with 3-nitrobenzyl alcohol as the matrix. Infra-red spectra were recorded as KBr discs on a Bruker IFS-66V spectrophotometer. Solid state electronic spectra were recorded on a Hitachi 4-3200 spectrophotometer using $MgCO_3$ as reference. Magnetic studies were determined at room temperature on a

* Corresponding author. Tel.: +34 986 812607; fax: +34 986 813797.
E-mail address: qilaura@uvigo.es (L. Valencia).

0022-328X/$ - see front matter © 2009 Elsevier B.V. All rights reserved.
doi:10.1016/j.jorganchem.2009.02.026

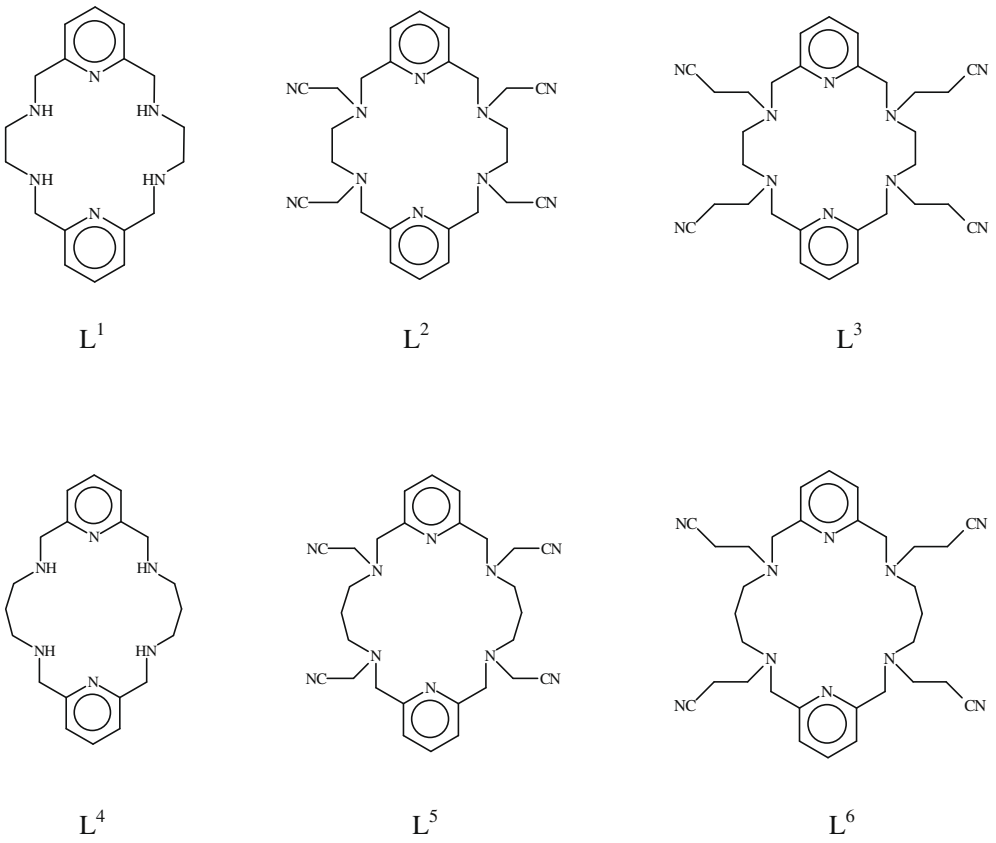

Scheme 1.

vibration sample magnetometer (VSM) Digital Measurement System 1660 with a magnetic field of 5000 G.

2.3. X-ray data collection, structure determination, and refinement

Slow recrystallization from acetonitrile gave crystals of $[MnL^1][MnBr_4]$, $[MnL^3][MnBr_4]\cdot 2CH_3CN$, $[Mn_2L^5Br_4]\cdot 2CH_3CN$ and $[Mn_2L^6Br_4]$ suitable for X-ray diffraction. The details of the X-ray crystal data, and the structure solution and refinement are given in Table 1. Measurements were made on a Bruker SMART CCD 1000 area diffractometer. All data were corrected for Lorentz and polarization effects. Empirical absorption corrections were also applied for all the crystal structures obtained [33]. Complex scattering factors were taken from the program package SHELXTL [34]. The structures were solved by direct methods which revealed the position of all non-hydrogen atoms. All the structures were refined on F^2 by a full-matrix least-squares procedure using anisotropic displacement parameters for all non-hydrogen atoms. The hydrogen atoms were located in their calculated positions and refined using a riding model.

2.4. Synthesis of metal complexes – general procedure

The $MnBr_2\cdot 4H_2O$ metal salt (0.40 mmol) was dissolved in acetonitrile (15 mL) and added to a stirred solution of the ligand, L^n (0.25 mmol) in acetonitrile (20 mL). The solution was stirred for 2 h and concentrated to the air at room temperature to obtain crystalline precipitates. The resulting products were filtered off, dried and recrystallized from acetonitrile.

2.4.1. $[MnL^1][MnBr_4]$ (**1**)

Anal. calc. for $C_{18}H_{26}N_6Br_4Mn_2$ (MW: 755.9): C, 27.6; H, 3.5; N, 11.1. Found: C, 27.7; H, 3.6; N, 10.9%. Yield: 47%. IR (KBr, cm^{-1}): 1614, 1579, 1473 [ν(C=N)$_{py}$ and ν(C=C)]. LSI-MS, m/z: 382 $[MnL^1]^+$, 375 $[MnBr_4]^+$. Color: pale pink.

2.4.2. $[MnL^2][MnBr_4]$ (**2**)

Anal. calc. for $C_{26}H_{30}N_{10}Br_4Mn_2$ (MW: 912.1): C, 34.4; H, 3.3; N, 15.4. Found: C, 34.1; H, 3.2; N, 15.2%. Yield: 39%. IR (KBr, cm^{-1}): 1609, 1583, 1456 [ν(C=N)$_{py}$ and ν(C=C)], 2252 [ν(C≡N)]. LSI-MS, m/z: 538 $[MnL^2]^+$, 375 $[MnBr_4]^+$. Color: pale pink.

2.4.3. $[MnL^3][MnBr_4]\cdot 2CH_3CN$ (**3**)

Anal. calc. for $C_{34}H_{44}N_{12}Br_4Mn_2$ (MW: 1050.3): C, 38.9; H, 4.2; N, 16.0. Found: C, 39.1; H, 4.3; N, 16.1%. Yield: 42%. IR (KBr, cm^{-1}): 1609, 1581, 1476 [ν(C=N)$_{py}$ and ν(C=C)], 2426, 2250 [ν(C≡N)]. LSI-MS, m/z: 594 $[MnL^3]^+$, 375 $[MnBr_4]^+$. Color: pale pink.

2.4.4. $[Mn_2L^4Br_4]$ (**4**)

Anal. calc. for $C_{20}H_{30}N_6Br_4Mn_2$ (MW: 784.0): C, 30.7; H, 3.9; N, 10.7. Found: C, 30.4; H, 3.7; N, 10.6%. Yield: 37%. IR (KBr, cm^{-1}): 1610, 1582, 1475 [ν(C=N)$_{py}$ and ν(C=C)]. LSI-MS, m/z: 785 $[Mn_2L^4Br_4]^+$, 625 $[Mn_2L^4Br_2]^+$, 465 $[Mn_2L^4]^+$. Color: pale pink.

2.4.5. $[Mn_2L^5Br_4]\cdot 2CH_3CN$ (**5**)

Anal. calc. for $C_{30}H_{40}N_{12}Br_4Mn_2$ (MW: 998.2): C, 36.1; H, 4.0; N, 16.8. Found: C, 35.9; H, 4.1; N, 16.6%. Yield: 41%. IR (KBr, cm^{-1}): 1616, 1579, 1474 [ν(C=N)$_{py}$ and ν(C=C)], 2251 [ν(C≡N)]. LSI-MS, m/z: 861 $[Mn_2L^5Br_3]^+$, 781 $[Mn_2L^5Br_2]^+$, 621 $[Mn_2L^5]^+$. Color: pale pink.

2.4.6. $[Mn_2L^6Br_4]$ (**6**)

Anal. calc. for $C_{32}H_{42}N_{10}Br_4Mn_2$ (MW: 997.2): C, 38.6; H, 4.2; N, 14.1. Found: C, 38.4; H, 4.0; N, 14.2%. Yield: 48%. IR (KBr, cm^{-1}): 1617, 1579, 1475 [ν(C=N)$_{py}$ and ν(C=C)], 2250 [ν(C≡N)]. LSI-MS,

Table 1
Crystal data and structure refinement for $[MnL^1][MnBr_4]$, $[MnL^3][MnBr_4]\cdot 2CH_3CN$, $[Mn_2L^5Br_4]\cdot 2CH_3CN$ and $[Mn_2L^6Br_4]$.

	$[MnL^1][MnBr_4]$	$[MnL^3][MnBr_4]\cdot 2CH_3CN$	$[Mn_2L^5Br_4]\cdot 2CH_3CN$	$[Mn_2L^6Br_4]$
Empirical formula	$C_{18}H_{26}N_6Br_4Mn_2$	$C_{68}H_{88}N_{24}Br_8Mn_2$	$C_{32}H_{40}N_{12}Br_4Mn_2$	$C_{32}H_{42}N_{10}Br_4Mn_2$
Formula weight	755.97	2100.66	1022.28	996.28
Temperature (K)	293(2)	120(2)	293(2)	293(2)
Wavelength (Å)	0.71073	0.71073	0.71073	0.71073
Crystal system	Monoclinic	Triclinic	Triclinic	Orthorombic
Space group	$P21/c$	$P\bar{1}$	$P\bar{1}$	$Pna2_1$
Unit cell dimensions				
a (Å)	10.6699(8)	11.205(2)	8.681(3)	16.352(2)
b (Å)	18.7147(13)	11.973(2)	11.050(4)	15.804(2)
c (Å)	14.2287(10)	17.060(3)	11.586	15.0231(18)
α (°)		94.198(4)	103.367(9)	
β (°)	110.352(2)	92.383(4)	98.926(7)	
γ (°)		112.503(4)	106.644(8)	
Volume (Å^3)	2663.9(3)	2102.9(7)	1006.3(7)	3882.4(8)
Z	4	1	1	4
Density (calculated) (Mg/m^3)	1.885	1.659	1.687	1.704
Absorption coefficient (mm^{-1})	6.964	4.441	4.637	4.804
$F(000)$	1464	1044	506	1976
Crystal size (mm^3)	0.25 × 0.15 × 0.13	0.26 × 0.14 × 0.07	0.22 × 0.21 × 0.11	0.21 × 0.11 × 0.10
Theta range for data collection (°)	1.87–21.60	1.85–23.81	1.86–23.81	1.79–22.72
Index ranges	$-11 \leqslant h \leqslant 11$, $-19 \leqslant k \leqslant 19$, $-8 \leqslant l \leqslant 14$	$-12 \leqslant h \leqslant 11$, $-13 \leqslant k \leqslant 13$, $-19 \leqslant l \leqslant 18$	$-9 \leqslant h \leqslant 9$, $-7 \leqslant k \leqslant 11$, $-13 \leqslant l \leqslant 11$	$-17 \leqslant h \leqslant 17$, $-17 \leqslant k \leqslant 15$, $-16 \leqslant l \leqslant 15$
Reflections collected	9406	8901	4341	14455
Independent reflections [$R_{(int)}$]	3039 [0.0477]	5745 [0.0546]	3979 [0.0625]	4957 [0.0939]
Completeness to theta	97.9% (21.60°)	88.8% (23.81°)	81% (23.81°)	99.4% (22.72°)
Absorption correction				
Maximum and minimum transmission	0.4646 and 0.2749	0.7463 and 0.3914	0.6295 and 0.4286	0.6451 and 0.4319
Refinement method	Full-matrix least-squares on F^2	Full-matrix least-squares on F^2	Full-matrix least-squares on F^2	Full-matrix least-squares on F^2
Data/restraints/parameters	3039/0/271	5745/0/471	2801/0/228	4957/13/433
Goodness-of-fit on F^2	0.881	0.751	0.860	0.675
Final R indices [$I > 2\sigma(I)$]	$R_1 = 0.0330$, $wR_2 = 0.0530$	$R_1 = 0.0494$, $wR_2 = 0.0781$	$R_1 = 0.0647$, $wR_2 = 0.1370$	$R_1 = 0.0426$, $wR_2 = 0.0498$
R indices (all data)	$R_1 = 0.0680$, $wR_2 = 0.0577$	$R_1 = 0.1328$, $wR_2 = 0.0936$	$R_1 = 0.1119$, $wR_2 = 0.1515$	$R_1 = 0.1193$, $wR_2 = 0.0634$
Absolute structure parameter				0.028(10)
Largest difference peak and hole (e Å^{-3})	0.679 and −0.56	0.974 and −0.393	1.1213 and −0.780	0.354 and −0.330

m/z: 998 $[Mn_2L^6Br_4]^+$, 916 $[Mn_2L^6Br_3]^+$, 677 $[Mn_2L^6]^+$. Color: pale pink.

3. Results and discussion

Mn(II) metal complexes of the L^n ligands were synthesized by reaction of the appropriate ligand and the bromide metal salt in refluxing acetonitrile. The complexes were synthesized as described in the Section 2 and, in general, the reactions gave analytically pure products. Complexes were characterized by elemental analysis, LSI mass spectrometry, IR, UV–Vis spectroscopy and magnetic measurements.

The IR spectra of the complexes show similar features. The ν(C=N) and ν(C=C) bands of the aromatic rings are generally shifted to higher wavenumbers than in the free ligand, suggesting the coordination to the metal ions [35].

The complexes with the ligands showing pendant-arms display a medium intensity band in the region 2250 cm^{-1} attributed to the ν(C≡N) mode, suggesting the no coordination of the nitrile groups to the metal. However, in the case of complex **3**, an additional band at 2426 cm^{-1} is observed, and can be attributable to the π,π-interaction in the solid state between py–CH_3CN–$CN_{pendant}$, similar to that found in other complexes with those ligands [36].

The results of LSI-MS of the complexes provide important evidence of the formation of the different nuclearity of the complexes as they feature peaks attributable in all cases to the species $[MnL^n]^+$ and $[MnBr_4]^+$ (n = 1–3) or $[Mn_2L^nBr_x]^+$ (n = 4–6).

The reflectance spectra of the complexes do not exhibit any band in the 250–2000 nm region, according to the absence of spin-allowed transitions for manganese(II). The value of the room temperature magnetic moments (by metal atom) is between 5.4–5.7 B.M., corresponding to high-spin state Mn (II).

3.1. X-ray structures

3.1.1. Crystal structure of $[MnL^1][MnBr_4]$ (**1**) and $[MnL^3][MnBr_4]\cdot 2CH_3CN$ (**3**)

By slow recrystallisation of the compounds $[MnL^1][MnBr_4]$ and $[MnL^3][MnBr_4]\cdot 2CH_3CN$ in acetonitrile, crystals to be studied by X-ray diffraction could be obtained. The molecular structures of the cationic complex are shown in Figs. 1 and 2a, respectively, together with the atomic numbering scheme adopted and selected bond distances (Å) and angles (°). Crystal data and structure refinement are given in Table 1.

Both complexes present a similar structure, consistent with the cationic complex $[MnL^n]^{2+}$ and a well separated $[MnBr_4]^{2-}$ anion.

In both cases the structure of the cation $[MnL^n]^{2+}$ shows the presence of a Mn(II) mononuclear complex, where the metal ion is endomacrocyclicly coordinated by the six N donor atoms from the macrocyclic framework. The coordination geometry around the Mn(II) ion can be described as $\{N_6\}$ distorted octahedral.

The equatorial plane can be described by the amine nitrogen atoms [N(2)–N(3)–N(5)–N(6), rms 0.6198 and 0.6153 for **1** and **3**, respectively], with the N atoms from the pyridine rings occupying the axial positions. The angles N(1)–Mn(1)–N(4), 167.01(19) and

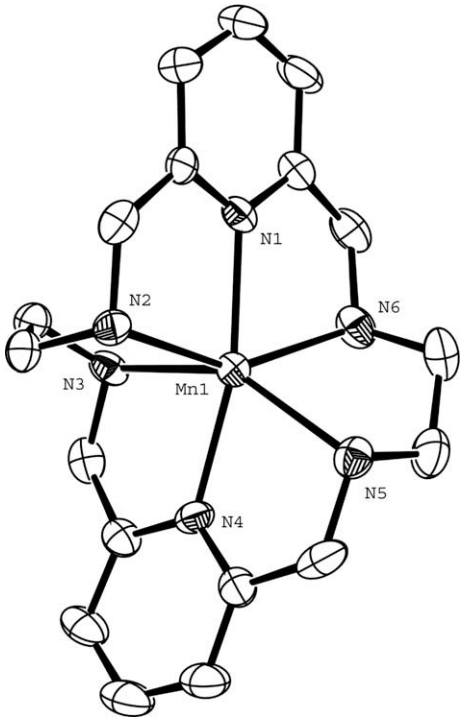

Fig. 1. Crystal structure of the cation complex $[MnL^1]^{2+}$; Selected bond lengths (Å) and angles (°): N(1)–Mn(1) 2.194(4); N(2)–Mn(1) 2.286(4); N(3)–Mn(1) 2.302(4); N(4)–Mn(1) 2.197(4); N(5)–Mn(1) 2.277(4); N(6)–Mn(1) 2.274(4); Mn(2)–Br(4) 2.4879(11); Mn(2)–Br(1) 2.4913(10); Mn(2)–Br(2) 2.4980(10); Mn(2)–Br(3) 2.4979(10); N(1)–Mn(1)–N(4) 167.01(19); N(1)–Mn(1)–N(6) 74.61(17); N(4)–Mn(1)–N(6) 112.90(16); N(1)–Mn(1)–N(5) 118.63(16); N(4)–Mn(1)–N(5) 73.94(18); N(6)–Mn(1)–N(5) 79.16(17); N(1)–Mn(1)–N(2) 74.87(17); N(4)–Mn(1)–N(2) 97.83(16); N(6)–Mn(1)–N(2) 149.22(16); N(5)–Mn(1)–N(2) 112.59(16); N(1)–Mn(1)–N(3) 93.41(15); N(4)–Mn(1)–N(3) 74.50(18); N(6)–Mn(1)–N(3) 106.23(17); N(5)–Mn(1)–N(3) 147.45(16); N(2)–Mn(1)–N(3) 79.51(16); Br(4)–Mn(2)–Br(1) 111.86(4); Br(4)–Mn(2)–Br(2) 114.12(4); Br(1)–Mn(2)–Br(2) 106.67(3); Br(4)–Mn(2)–Br(3) 106.71(4); Br(1)–Mn(2)–Br(3) 109.86(4); Br(2)–Mn(2)–Br(3) 107.52(4).

176.5(3)° for **1** and **3**, respectively, show that the macrocycle ligand is slightly folded in both cases.

The ligand adops a typical "twist-wrap" conformation with a dihedral plane between pyridine rings of 84.2(2) for **1** and 82.1(2)° for **3**.

The different electronic nature of the N donor atoms induces also geometrical distortions from the ideal octahedral geometry, which are manifested by significantly different Mn–N bond lengths. The shortest bond distances between the metal ion and the donor atoms belong to the pyridinic nitrogen, with an average value Mn–N_{py} of 2.195 and 2.139 Å for **1** and **3**, respectively. The Mn–N_{am} bond lengths are similar in both complexes, with an average value of 2.2818 and 2.3283 Å for **1** and **3**, respectively, and they are in the order to that found for similar complexes of Mn(II) [37–39].

The $[MnBr_4]^{2-}$ anion lies in a general position within the unit cell and it presents a roughly tetrahedral symmetry typical for this specie [40,41]. The Mn–Br bond distances are in the range 2.4879(11)–2.4989(10) Å for **1**, and 2.4888(17)–2.5275(16) Å for **3**. The Br–Mn–Br angles are in the range 106.67(3)–114.12(4) and 105.51(6)–116.62(6)° for **1** and **3**, respectively.

In the case of the $[MnL^3]^{2+}$ cation complex, the nitrile groups are no coordinated to the manganese ion, probably due to their linear nature, as has been found in other previously related crystal structures [17–20]. However, intramolecular interactions between the π-systems of the pyridine rings, the nitrile pendant-arms and the acetonitrile solvent molecules, can be observed (Fig. 2b) [36].

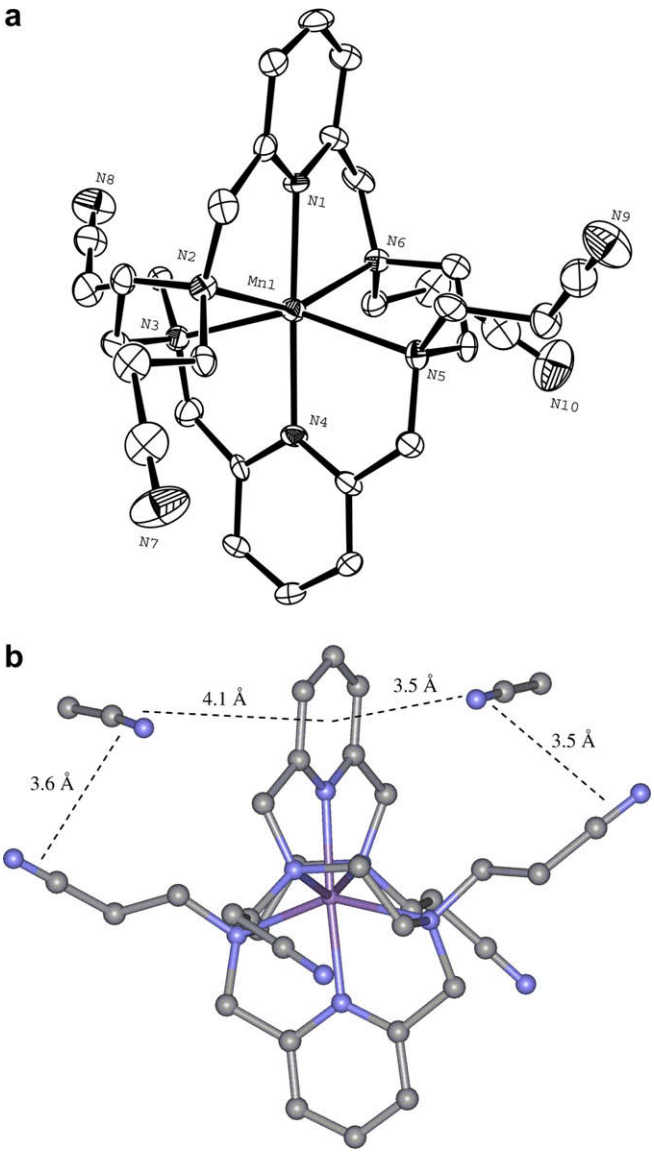

Fig. 2. (a) Crystal structure of the cation complex $[MnL^3]^{2+}$; Selected bond lengths (Å) and angles (°): N(1)–Mn(1) 2.143(6); N(2)–Mn(1) 2.285(6); N(3)–Mn(1) 2.335(7); N(4)–Mn(1) 2.135(6); N(5)–Mn(1) 2.362(6); N(6)–Mn(1) 2.331(6); Mn(2)–Br(4) 2.4888(17); Mn(2)–Br(5) 2.4988(16); Mn(2)–Br(3) 2.5058(18); Mn(2)–Br(1) 2.5275(16); N(4)–Mn(1)–N(1) 176.5(3); N(4)–Mn(1)–N(2) 104.1(2); N(1)–Mn(1)–N(2) 74.7(2); N(4)–Mn(1)–N(6) 106.7(2); N(1)–Mn(1)–N(6) 74.5(2); N(2)–Mn(1)–N(6) 149.2(2); N(4)–Mn(1)–N(3) 75.4(3); N(1)–Mn(1)–N(3) 107.5(2); N(2)–Mn(1)–N(3) 81.9(2); N(6)–Mn(1)–N(3) 106.6(2); N(4)–Mn(1)–N(5) 74.2(3); N(1)–Mn(1)–N(5) 102.8(2); N(2)–Mn(1)–N(5) 106.2(2); N(6)–Mn(1)–N(5) 81.7(2); N(3)–Mn(1)–N(5) 149.6(2); Br(4)–Mn(2)–Br(5) 112.06(6); Br(4)–Mn(2)–Br(3) 111.41(6); Br(5)–Mn(2)–Br(3) 105.53(6); Br(4)–Mn(2)–Br(1) 105.68(6); Br(5)–Mn(2)–Br(1) 105.51(6); Br(3)–Mn(2)–Br(1) 116.62(6). (b) Crystal structure of $[MnL^3]^{2+} \cdot 2CH_3CN$ showing the π,π-interactions between nitrile pendant-arms, acetonitrile solvent molecules and pyridine ring.

The crystal lattice of **3** shows the presence of two acetonitrile molecules near of one the pyridine rings and the nitrile pendants of the ligand. One of these acetonitrile solvent molecule is sited between the pyridine ring and one nitrile pendant group, with a $d_{centroid-C\equiv N}$ and $d_{C\equiv N-C\equiv N}$ of 3.5 Å, in both cases. If we consider the distance between the centroid of the pyridine ring and the C≡N groups of the nitrile pendant and the acetonitrile molecules, as analogous to the centroid–centroid distance, these distances should be considered as indicative of the presence of intramolecular π,π-interactions. The second acetonitrile molecule shows $d_{C\equiv N-C\equiv N}$ and $d_{centroid-C\equiv N}$ distances of 3.6 and 4.1 Å, respectively,

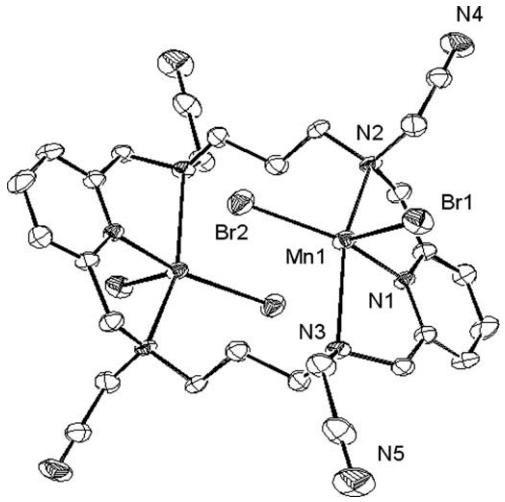

Fig. 3. Crystal structure of $[Mn_2L^5Br_4]\cdot 2CH_3CN$; Selected bond lengths (Å) and angles (°): N(1)–Mn(1) 2.167(7); N(2)–Mn(1) 2.443(6); N(3)–Mn(1) 2.431(6); Mn(1)–Br(2) 2.4857(18); Mn(1)–Br(1) 2.5162(18); N(1)–Mn(1)–N(3) 72.9(2); N(1)–Mn(1)–N(2) 73.1(2); N(3)–Mn(1)–N(2) 143.4(2); N(1)–Mn(1)–Br(2) 152.50(18); N(3)–Mn(1)–Br(2) 104.29(18); N(2)–Mn(1)–Br(2) 99.52(16); N(1)–Mn(1)–Br(1) 100.47(18); N(3)–Mn(1)–Br(1) 95.47(17); N(2)–Mn(1)–Br(1) 103.68(17); Br(2)–Mn(1)–Br(1) 107.02(7).

showing the possible π,π-interaction between the acetonitrile molecule and nitrile pendant group, but too long between the acetonitrile molecule and pyridine ring for it.

*3.1.2. Crystal structure of $[Mn_2L^5Br_4]\cdot 2CH_3CN$ (**5**) and $[Mn_2L^6Br_4]$ (**6**)*

By slow concentration of acetonitrile solutions, crystals suitable for X-ray diffraction of $[Mn_2L^5Br_4]\cdot 2CH_3CN$ and $[Mn_2L^6Br_4]$ were obtained. The molecular structure together with selected bond lengths (Å) and angles (°) are given in Figs. 3 and 4, respectively. The crystal data and structure refinement are given in Table 1.

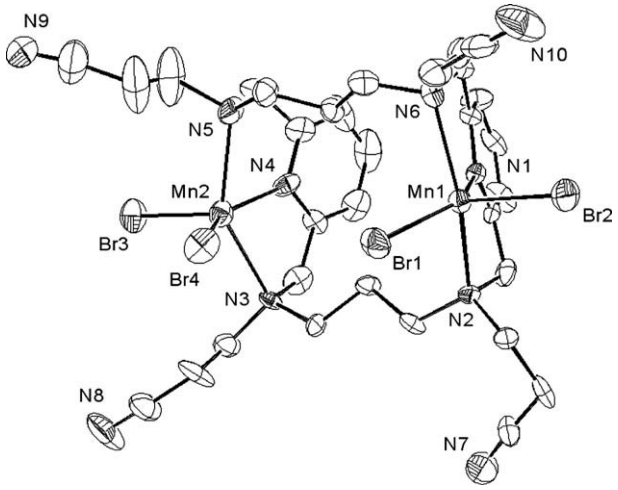

Fig. 4. Crystal structure of $[Mn_2L^6Br_4]$; Selected bond lengths (Å) and angles (°): Br(1)–Mn(1) 2.4709(19); Br(2)–Mn(1) 2.4826(19); Br(3)–Mn(2) 2.5002(19); Br(4)–Mn(2) 2.488(2); Mn(1)–N(1) 2.143(9); Mn(1)–N(6) 2.361(9); Mn(1)–N(2) 2.392(8); Mn(2)–N(4) 2.111(11); Mn(2)–N(5) 2.380(9); Mn(2)–N(3) 2.399(8); N(1)–Mn(1)–N(6) 75.2(3); N(1)–Mn(1)–N(2) 75.2(3); N(6)–Mn(1)–N(2) 146.8(3); N(1)–Mn(1)–Br(1) 143.5(2); N(6)–Mn(1)–Br(1) 100.0(2); N(2)–Mn(1)–Br(1) 94.8(2); N(1)–Mn(1)–Br(2) 107.6(2); N(6)–Mn(1)–Br(2) 100.1(2); N(2)–Mn(1)–Br(2) 103.0(2); Br(1)–Mn(1)–Br(2) 108.88(7); N(4)–Mn(2)–N(5) 74.6(4); N(4)–Mn(2)–N(3) 75.7(4); N(5)–Mn(2)–N(3) 145.5(4); N(4)–Mn(2)–Br(4) 142.2(3); N(5)–Mn(2)–Br(4) 96.3(3); N(3)–Mn(2)–Br(4) 96.4(2); N(4)–Mn(2)–Br(3) 104.5(3); N(5)–Mn(2)–Br(3) 101.6(2); N(3)–Mn(2)–Br(3) 102.5(2); Br(4)–Mn(2)–Br(3) 113.30(9).

In both cases, the complexes are neutral and dinuclear. The Mn(II) ions are endomacrocyclic coordinated in a $\{N_3Br_2\}$ core by one pyridinic nitrogen atom, the two contiguous amine groups to this pyridine ring and two bromide atoms. For **5**, the asymmetric unity shows only half molecule of the Mn(II) complex, and the environment around the manganese atom can be better described as distorted square pyramidal with $\tau = 0.16$, where the Br(1) is occupying the apex of the pyramid. For **6**, the environment around each manganese atom is also better described as distorted square pyramidal with $\tau = 0.06$ for Mn(1) and Mn(2). In this case, Br(2) and Br(3) are occupying the apex of the pyramid for the Mn(1) and Mn(2) environment, respectively.

The distance between the manganese ions, 5.345 and 6.03 Å for **5** and **6**, respectively, indicates the no interaction between metal ions.

The pyridinic nitrogen atom provides the shortest bond distance to the manganese atom for both complexes, with N(1)–Mn(1) of 2.167(7) Å for **5** and N(1)–Mn(1) 2.143(9) Å or N(4)–Mn(2) 2.111(11) Å for **6**. The aliphatic Mn–N bond distances vary from 2.377 Å [average value for Mn(1) in **6**] to 2.437 Å [average value for **5**]. The Mn–Br distances are in the range 2.4709(19)–2.5162(18) Å, and they are consistent with the values observed in other similar pentacoordinated manganese complexes [42,43].

In both cases, the crystal structure shows that the macrocyclic ligands are no twisted, but in **5** the ligand presents a step conformation with the pyridine rings parallel to one another and a dihedral angles of 71° to the plane described by the four tertiary amine nitrogen atoms. Instead in **6**, the macrocycle ligand is folded, with a dihedral angle 33.8° between the pyridine rings and a distance between centroids of 4.1 Å, too long to be considered as π,π-interaction.

4. Conclusion

The complexation capability of a series of azamacrocyclic ligands – some of them containing nitrile groups as pendant-arms – towards Mn(II) bromide salt have been studied. The crystal structure $[MnL^1][MnBr_4]$, $[MnL^3][MnBr_4]\cdot 2CH_3CN$, $[Mn_2L^5Br_4]\cdot 2CH_3CN$ and $[Mn_2L^6Br_4]$ complexes have been determined. In all cases the ligands are bounded to the metal ions by the nitrogen donor set of the macrocyclic backbone, remaining the nitrile pendant-arms without participating in the coordination. The Mn(II) complexes with the ligands L^1 and L^3 present an ionic mixed octahedral–tetrahedral complex. The manganese ion is endomacrocyclicly coordinated in an N_6 octahedral geometry in the mononuclear cation complex. Instead, the complexes with L^5 and L^6 are neutral and dinuclear, with the metal ions in N_3Br_2 distorted square pyramidal environment. In the case of complex $[MnL^3][MnBr_4]\cdot 2CH_3CN$, the presence of intramolecular π,π-interactions between pyridine ring, an acetonitrile molecule and nitrile pendant group can be also observed.

5. Supplementary material

CCDC 720558, 720559, 720560 and 720561 contain the supplementary crystallographic data for $[MnL^1][MnBr_4]$, $[MnL^3][MnBr_4]\cdot 2CH_3CN$, $[Mn_2L^5Br_4]\cdot 2CH_3CN$ and $[Mn_2L^6Br_4]$. These data can be obtained free of charge from The Cambridge Crystallographic Data Centre via www.ccdc.cam.ac.uk/data_request/cif.

Acknowledgments

We thank Xunta de Galicia (PGIDT01PXI20901PR) and Universidade de Vigo (1Z1464102) for financial support. Intensity mea-

surements were performed at the Servicio de Rayos X. CACTI. Universidade de Vigo.

References

[1] P. Guerriero, S. Tamburini, P.A. Vigato, Coord. Chem. Rev. 139 (1995) 17. and references therein.
[2] S.-G. Kang, N.-S. Kim, J.-S. Choi, D. Whang, K. Kim, J. Chem. Soc., Dalton Trans. (1995) 363.
[3] E. Kimura, Y. Kodake, M. Shionya, M. Shiro, Inorg. Chem. 29 (1990) 4991.
[4] K. Hiate, M. Mikuriya, J. Chem. Soc., Dalton Trans. (1990) 2763.
[5] S.-K. Jung, S.-G. Kang, M.P. Suh, Bull. Kor. Chem. Soc. 10 (1989) 362.
[6] S.W.A. Bligh, N. Choi, C.F.G.C. Geraldes, S. Knoke, M. Mc Partlin, M.J. Sanganee, T.M. Woodroffe, J. Chem. Soc., Dalton Trans. (1997) 4119.
[7] S.W.A. Bligh, N. Choi, W.J. Cummins, E.G. Evagorou, J.D. Kelly, M. Mc Partlin, J. Chem. Soc., Dalton Trans. (1993) 3829.
[8] L. Valencia, J. Martínez, A. Macías, R. Bastida, R.A. Carvalho, C.F.G.C. Geraldes, Inorg. Chem. 41 (2002) 5300.
[9] L. Valencia, R. Bastida, M. López-Deber, A. Macías, A. Rodríguez, M. Vicente, Z. Anorg. Allg. Chem. 629 (2003) 268.
[10] R. Bastida, D.E. Fenton, M. López-Deber, A. Macías, L. Valencia, M. Vicente, Inorg. Chim. Acta 355 (2003) 292.
[11] L. Valencia, R. Bastida, A. Macías, M. Vicente, P. Pérez-Lourido, New J. Chem. 29 (2005) 424.
[12] J. Martínez, R. Bastida, A. Macías, L. Valencia, M. Vicente, Z. Anorg. Allg. Chem. 631 (2005) 2046.
[13] Mª del C. Fernández-Fernández, R. Bastida, A. Macías, L. Valencia, P. Pérez-Lourido, Polyhedron 25 (2006) 783.
[14] Mª del C. Fernández-Fernández, R. Bastida, A. Macías, P. Pérez-Lourido, C. Platas-Iglesias, L. Valencia, Inorg. Chem. 45 (2006) 4484.
[15] C. Núñez, R. Bastida, A. Macías, M. Mato-Iglesias, C. Platas-Iglesias, L. Valencia, Dalton Trans. (2008) 3841.
[16] L. Valencia, P. Pérez-Lourido, R. Bastida, A. Macías, Cryst. Growth Des. 8 (2008) 2080.
[17] S. González, L. Valencia, R. Bastida, D.E. Fenton, A. Macías, A. Rodríguez, J. Chem. Soc., Dalton Trans. (2002) 3551.
[18] L. Valencia, R. Bastida, Mª del C. Fernández-Fernández, A. Macías, M. Vicente, Inorg. Chim. Acta 358 (2005) 2618.
[19] Mª del C. Fernández-Fernández, R. Bastida, A. Macías, P. Pérez-Lourido, L. Valencia, Inorg. Chem. 45 (2006) 2266.
[20] Mª del C. Fernández-Fernández, R. Bastida, A. Macías, P. Pérez-Lourido, L. Valencia, Polyhedron 26 (2007) 5317.
[21] E.C. Samudo, V.A. Grillo, M.J. Knapp, J.C. Bollinger, J.C. Huffman, D.N. Hendrickson, G. Christou, Inorg. Chem. 41 (2002) 2441.
[22] R. Shimanovich, S. Hannah, V. Lynch, N. Gerasimchuck, T.D. Mody, D. Magda, J. Sessler, J.T. Groves, J. Am. Chem. Soc. 123 (2001) 3613.
[23] T. Wieprecht, J. Xia, U. Heinz, J. Dannacher, G. Schlingloff, J. Mol. Catal. A 203 (2003) 113. and references therein.
[24] A.L. Schwartz, E. Yikilmaz, C.K. Vance, S. Vathyam, R.L. Koder, A.-F. Miller, J. Inorg. Biochem. 80 (2000) 247.
[25] S.K. Smoukov, J. Telser, B.A. Bernat, C.L. Rife, R.N. Armstrong, B.M. Hoffman, J. Am. Chem. Soc. 124 (2002) 2318.
[26] A. Sigel, H. Sigel, Manganese and its Role in Biological Processes, Marcel Dekker, New York, 2000. p. 37.
[27] S.V. Antonyuk, V.R. Melik-Adamyan, A.N. Popov, V.S. Lamzin, P.D. Hempstead, P.M. Harrison, P.J. Artymyuk, V.V. Barynin, Crystallogr. Rep. 45 (2000) 105.
[28] V.V. Barynin, M.M. Whittaker, S.V. Antonyuk, V.S. Lamzin, P.V. Harrison, P.J. Artymyuk, V.J. Whittaker, Structure 9 (2001) 725.
[29] A. Zouni, H.T. Witt, J. Kern, P. Fromme, N. Krauss, W. Saenger, P. Orth, Nature 409 (2001) 739.
[30] N. Kamiya, J.-R. Shen, Proc. Natl. Acad. Sci. USA 100 (2003) 98.
[31] G.L. Rothermel Jr., L. Miao, A.L. Hill, S.C. Jackels, Inorg. Chem. 31 (1992) 4854.
[32] K.I. Dhont, W. Lippens, G.G. Herman, A.M. Goemine, Bull. Soc. Chim. Belg. 101 (1992) 1061.
[33] G.M. Sheldrick, SADABS Program for Empirical Absorption Correction of Area Detector Data, University of Göttingen, Germany, 1996.
[34] SHELXTL Version, An Integrated System for Solving and Refining Crystal Structures from Diffraction Data (Revision 5.1), Bruker AXS Ltd., Madison, Wis., USA, 1997.
[35] N.S. Gill, R.H. Nuttall, D.E. Scaife, D.W. Sharp, J. Inorg. Nucl. Chem. 18 (1961) 3091.
[36] L. Valencia Matarranz, R. Bastida, A. Macías, P. Pérez-Lourido, Polyhedron 27 (2008) 3509.
[37] X.-H. Bu, W. Chen, L.-J. Mu, Z.-H. Zhang, R.-H. Zhang, T. Clifford, Polyhedron 19 (2000) 2095.
[38] W. Park, M.H. Shin, J.H. Chung, J. Park, M.S. Lah, D. Lim, Tetrahedron Lett. 47 (2006) 8841.
[39] N. Arulsamy, J. Glerup, D.J. Hodgson, Inorg. Chem. 33 (1994) 3043.
[40] N.S. Fender, S.A. Finegan, D. Miller, M. Mitchell, I.A. Kahwa, F.R. Fronczek, Inorg. Chem. 33 (1994) 4002.
[41] N.S. Fender, F.R. Fronczek, V. John, I.A. Kahwa, G.L. McPherson, Inorg. Chem. 36 (1997) 5539.
[42] C. Mantel, C. Baffert, I. Romero, A. Deronzier, J. Pécaut, M.-N. Collomb, C. Duboc, Inorg. Chem. 43 (2004) 6455.
[43] X. Sala, A.M. Rodríguez, M. Rodríguez, I. Romero, T. Parella, A. Von Zelewsky, A. Llobet, J. Benet-Buchholz, J. Org. Chem. 71 (2006) 9283.